Electronic Supplementary Information

for

$^1J_{CH}$ couplings in Group14/IVA tetramethyls from the gas-phase NMR and DFT structural study: a search for the best computational protocol

Ryszard B. Nazarski*[a] and Włodzimierz Makulski[b]

[a]*Laboratory of Molecular Spectroscopy, Faculty of Chemistry, University of Łódź, Tamka 12, 91-403 Łódź, Poland*
[b]*Laboratory of NMR Spectroscopy, Faculty of Chemistry, University of Warsaw, Pasteura 1, 02-093 Warsaw, Poland*

E-mail: nazarski@uni.lodz.pl

Contents:

Table S1. Selected B3LYP/basis sets combinations tested (two steps considered) [a]

#	Geometry optimizations		*J*-coupling calculations		R^2 for $\nu_{as}(CH_3)$ = *f* [$\omega_{as}(CH_3)$]	R^2 for $^1J_{0,CH}$ = *f* ($^1J_{CH}^{theor}$)	Notes
	Basis set for the E atom	Basis set for C and H atoms	Basis set for the E atom	Basis set for C and H atoms			
1	**F**	**D**	**O**	**G**	0.9924	0.9650	b
2	**F**	**D**	**O**	**G**	0.9929	0.9658	
3	**A**	**D**	**L**	**G**	0.9987	0.9690	b
4	**A**	**D**	**L**	**G**	0.9973	0.9807	
5	**M**	**M**	**M**	**G**	0.9959	0.9783	
6	**A**	**C**	**L**	**G**	0.9982	0.9815	b, c
7	**A**	**C**	**M**	**I**	0.9994	0.9844	
8	**A**	**C**	**L**	**J**	0.9994	0.9845	
9	**A**	**C**	**L**	**G**	0.9994	0.9847	Protocol I
10	**B**	**C**	**M**	**I**	0.9998	0.9834	
11	**B**	**C**	**M**	**J**	0.9998	0.9840	
12	**B**	**C**	**M**	**G**	0.9998	0.9879	Protocol II
13	**B**	**D**	**M**	**G**	0.9970	0.9845	b
14	**B**	**D**	**M**	**G**	0.9967	0.9848	

[a] The gas-phase results for the all five species EMe_4. [b] The six Cartesian *d* functions have been employed (6D option). [c] Without the keyword 'Int=UltraFine'.

Notation of all basis sets used in this work:

A	def2-TZVPP
B	def2-TZVPPD
C	6-31G(*d*,*p*)
D	6-31+G(*d*,*p*)
E	6-31+G(2*df*,*p*)
F	aug-cc-pVTZ *or* aug-cc-pVTZ-PP (Sn, Pb)
G	IGLO-II
H	IGLO-III
I	aug-cc-pVTZ-J
J	pcJ-2
K	pcJ-3
L	def2-QZVPP
M	def2-QZVPPD
N	cc-pVQZ *or* cc-pVQZ-PP (Sn, Pb)
O	aug-cc-pVQZ *or* aug-cc-pVQZ-PP (Sn, Pb)

Table S2. *In vacuo* computed r_e *vs*. experimental r_g (from the GED data)[a-e] intramolecular distances in all five species **E**Me$_4$, [Å]

	r_g [a-e]	r_e [f]	$r_{e,scal}$ [f,g]	$r_g - r_{e,scal}$	$r_{e,lit}$ [h]	$r_e - r_{e,lit}$
C–C [a]	1.537	1.536	1.540	-0.003	1.537	-0.001
C–H	1.114	1.096	1.103	0.011		
1,3 C···H	2.200	2.184	2.183	0.017		
C···C	2.508	2.508	2.505	0.003		
1,4 C···H	2.767	2.761	2.756	0.011		
1,4 C···H	3.480	3.474	3.463	0.017		
Si–C [b]	1.877	1.882	1.884	-0.007	1.896	-0.014
C–H	1.110	1.096	1.104	0.007		
Si···H	2.500	2.501	2.498	0.002		
C···C	3.065	3.074	3.066	-0.001		
1,4 C···H	3.293	3.294	3.285	0.008		
1,4 C···H	4.031	4.035	4.021	0.011		
Ge–C [c]	1.958	1.976	1.977	-0.019	1.969	0.007
C–H	1.111	1.094	1.102	0.009		
Ge···H	2.570	2.577	2.573	-0.003		
C···C	3.198	3.226	3.218	-0.020		
Sn–C [d]	2.144	2.168	2.168	-0.024	2.172	-0.004
C–H	1.118	1.094	1.101	0.017		
Sn···H	2.764	2.749	2.744	0.020		
Pb–C [e]	2.238	2.258	2.256	-0.018	2.256	0.002
C–H	1.083 [i]	1.092	1.100	-0.017		
Pb···H [k]	[2.721] [j]	[2.817]	[2.807]	[-0.086]		
C···C	3.656	3.687	3.675	-0.019		

[a] Ref. 1. [b] Ref. 2. [c] Ref. 3. [d] Ref. 4. [e] Ref. 5. [f] This work (protocol II). [g] Corrected (scaled) r_e values computed with the equation $r_{e,scal} = (r_e + 0.01584)/1.0076$; see also Fig. S2. [h] B3LYP/RESC-derived E–C bond lengths, ref. 6. [i] This r_g distance seems to be underestimated, in the light of the C–H bond lengths in other species EMe$_4$. [j] Most likely strongly underestimated value. [k] This distance was not used in the least squares regression analysis.

Table S3. *In vacuo* computed $\omega_{as}(CH_3)$ *vs*. gas-phase experimental $\nu_{as}(CH_3)$ (from IR spectra)[a-c] C–H vibrational stretching fundamentals for all five species EMe$_4$, [cm^{-1}]

Compound	$\nu_{as}(CH_3)$ [a]	$\omega_{as}(CH_3)$ [d]	$\omega_{as}(CH_3)_{scal}$ [d,e]	$\nu_{as}(CH_3) - \omega_{as}(CH_3)_{scal}$	other $\nu_{as}(CH_3)$s
CMe_4	2960.7 [f]	3104.93	2960.71	0.0	2962,[b] 2959[c]
$SiMe_4$	2964.2	3109.12	2964.18	0.0	
$GeMe_4$	2980.6	3128.63	2980.34	0.3	
$SnMe_4$	2986.5	3136.49	2986.86	-0.4	
$PbMe_4$	3005.0	3158.27	3004.91	0.1	

[a] Ref. 7. [b] Ref. 8. [c] Ref. 9. [d] This work (protocol II). [e] Corrected (scaled) $\omega_{as}(CH_3)$ values computed applying the equation $\omega_{as}(CH_3)_{scal} = [\omega_{as}(CH_3) + 468.34]/1.2069$; see also Fig. S3. [f] The second (?) value at 2967.5 cm^{-1} has also been originally given for this fundamental frequency,[a] which was omitted in the current analysis.

Table S4. Computed[a] *vs*. observed $^1J_{CH}$ couplings for species EMe_4 in vacuum[b] and in CCl_4 or C_6H_6 solution,[c] together with their decomposition into all four Ramsey terms, [Hz]

Compound	Medium	FC	SD	PSO	DSO	Total J^{theor}	$^1J_{CH}$[b,c,d]
CMe_4	gas (I)	119.67	0.19	0.92	0.73	121.50	123.93(4)
	gas (II)	119.70	0.18	0.92	0.73	121.52	
	CCl_4 (I)	119.65	0.19	0.92	0.73	121.48	124.0(2)
	CCl_4 (II)	119.67	0.18	0.92	0.73	121.50	
	C_6H_6 (II)	119.67	0.18	0.92	0.73	121.50	124.3
$SiMe_4$	gas (I)	114.45	0.29	1.46	0.68	116.88	117.88(4)
	gas (II)	114.25	0.29	1.46	0.68	116.68	
	CCl_4 (I)	114.44	0.29	1.46	0.68	116.87	117.8(2)
	CCl_4 (II)	114.24	0.29	1.46	0.68	116.67	
	C_6H_6 (II)	114.24	0.29	1.46	0.68	116.66	118.2
$GeMe_4$	gas (I)	120.84	0.33	1.13	0.98	123.27	124.05(1)
	gas (II)	120.70	0.33	1.13	0.98	123.13	
	CCl_4 (I)	120.82	0.33	1.13	0.98	123.25	124.6(2)
	CCl_4 (II)	120.67	0.33	1.13	0.98	123.10	
	C_6H_6 (II)	120.67	0.33	1.13	0.98	123.10	124.4
$SnMe_4$	gas (I)	124.30	0.39	1.21	0.63	126.53	127.13(5)
	gas (II)	124.15	0.39	1.21	0.63	126.38	
	CCl_4 (I)	124.23	0.39	1.22	0.63	126.46	127.8(2)
	CCl_4 (II)	124.08	0.39	1.22	0.63	126.31	
	C_6H_6 (II)	124.08	0.39	1.22	0.63	126.31	127.7
$PbMe_4$	gas (I)	130.67	0.44	1.10	0.57	132.79	133.29(3)
	gas (II)	130.51	0.44	1.10	0.57	132.62	
	CCl_4 (I)	130.57	0.44	1.11	0.57	132.69	134.3(2)
	CCl_4 (II)	130.41	0.44	1.11	0.57	132.53	
	C_6H_6 (II)	130.41	0.44	1.11	0.57	132.53	134.2

[a] Protocol I, II, I-CCl_4, II-CCl_4, and II-C_6H_6 was applied, respectively. [b] The experimental $^1J_{0,CH,av}$ values from Table 1 (in the main text) were used as *in vacuo* data. [c] The data for ~10% CCl_4 solution from ^{1}H NMR spectra, according to ref. 10.[d] The data for ~10% C_6H_6 solution from $^{13}C\{^1H\}$ NMR spectra, according to ref. 11.

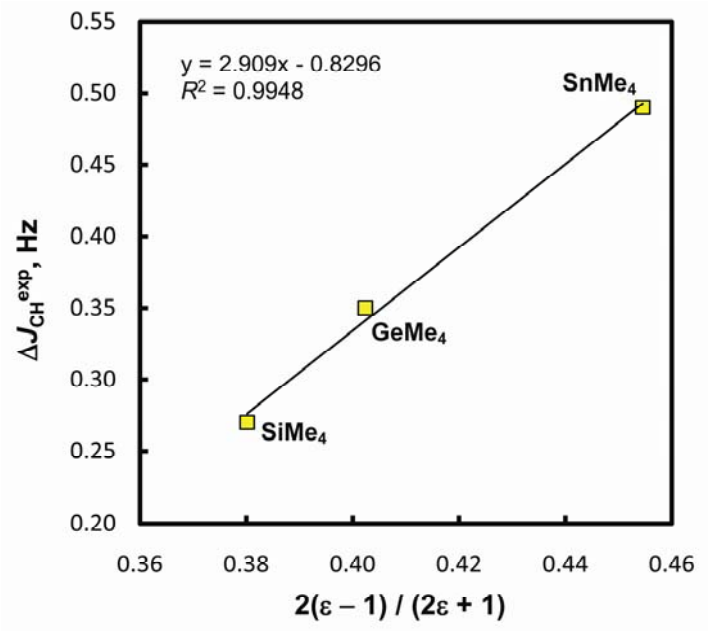

Fig. S1. Dependence of $\Delta^1J_{CH}^{exp} = {}^1J_{CH}(neat) - {}^1J_{0,CH,av}(gas)$ on the reaction field function of relative permittivity ε for the three normally liquid tetramethyls; *J* data from Table 1 (main text) and ε values from ref. 12 were used.

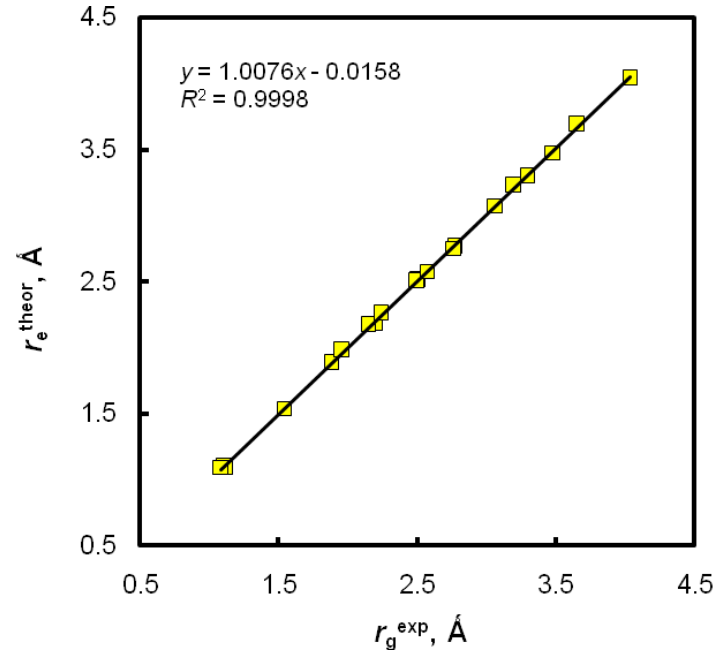

Fig. S2. Plot of computed (protocol II) r_e bond lengths *vs.* related experimental r_g distances for all five species EMe_4; the numeral data from Table S2 were used.

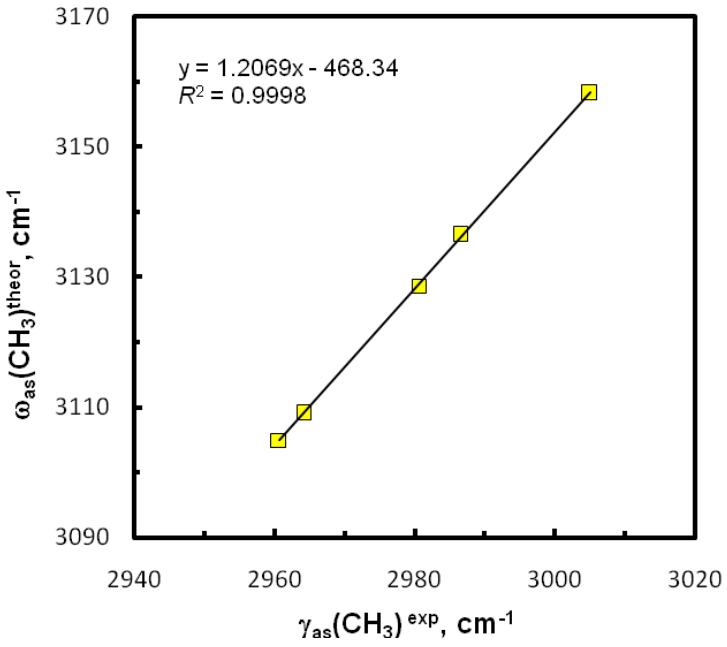

Fig. S3. Plot of *in vacuo* computed (protocol II) harmonic $\omega_{as}(CH_3)$s *vs*. experimental gas-phase frequencies, $\nu_{as}(CH_3)$s, for all five species EMe_4; the data from Table S3 were applied.

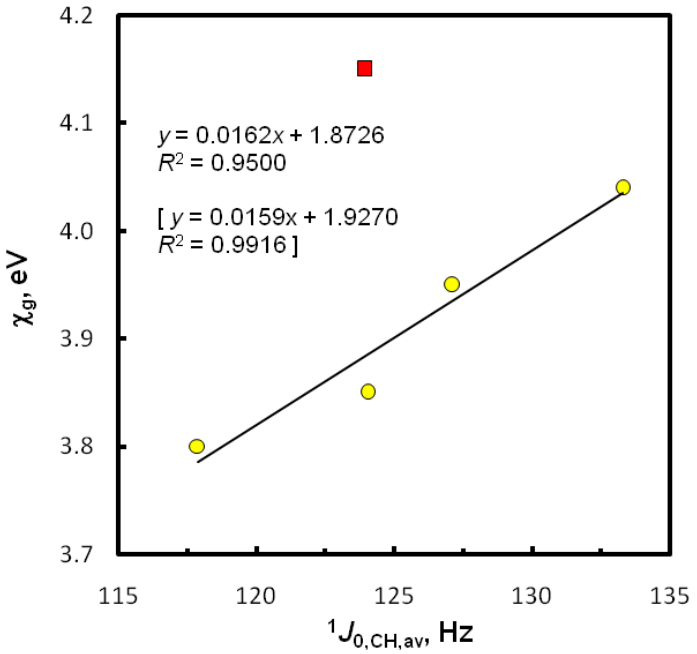

Fig. S4. The group electronegativity χ_g *vs*. experimental $^1J_{0,CH,av}$(gas) values; the CMe_4 data point (■) was omitted. Statistics with the χ_g corrected for $GeMe_4$ (3.88 eV) are in the bracket. The numeral data from Tables 1 and 3 (main text) were used.

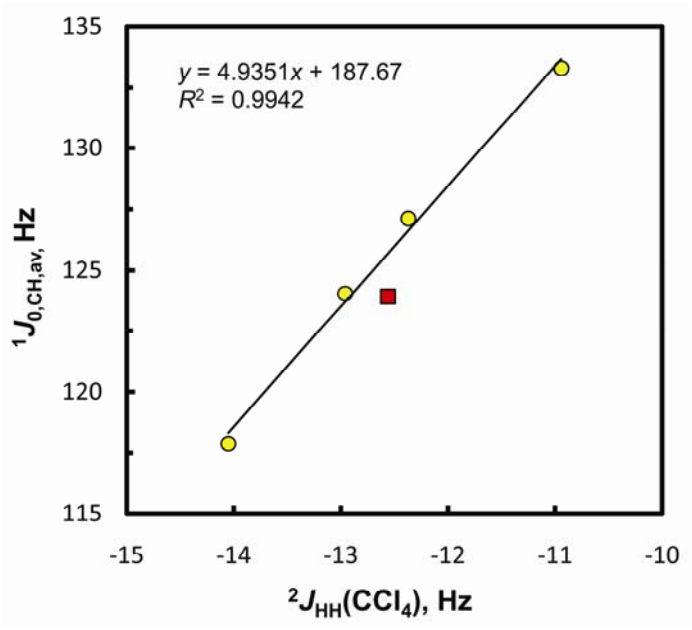

Fig. S5. Plot of experimental $^{1}J_{0,CH,av}$(gas) *vs.* $^{2}J_{HH}(CCl_4)$ values; the CMe_4 point (■) was omitted. The data from Tables 1 and 3 (main text) were applied.

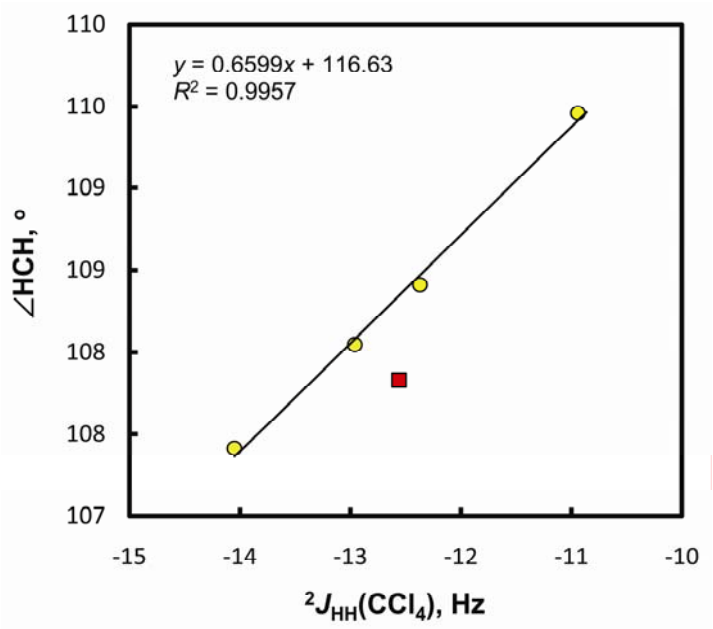

Fig. S6. Plot of the computed (protocol II) HCH bond angles *vs.* experimental $^{2}J_{HH}(CCl_4)$ couplings; the CMe_4 point (■) was omitted. The data from Table 3 (main text) were used.

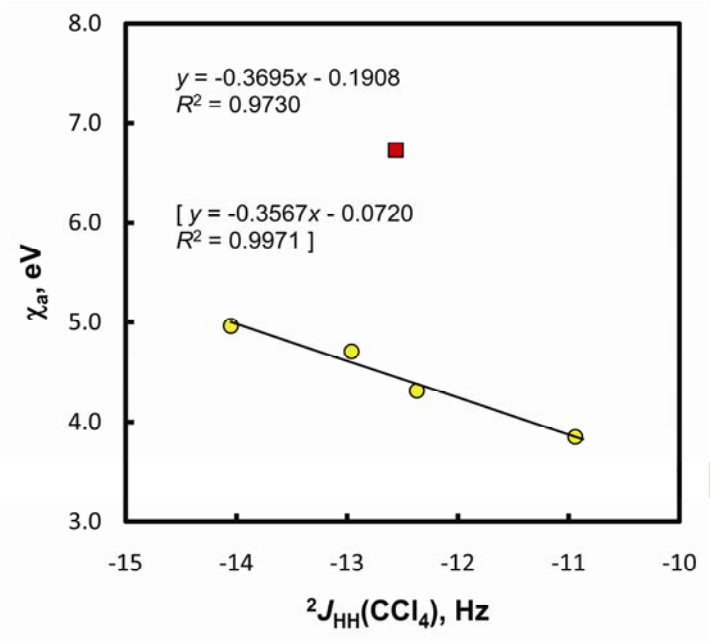

Fig. S7. The atom electronegativity χ_a *vs.* experimental $^2J_{HH}(CCl_4)$ couplings; the CMe_4 point (■) was omitted. Statistics with the χ_a corrected for Ge (4.54 eV) are in the bracket. The data from Table 3 (main text) were used.

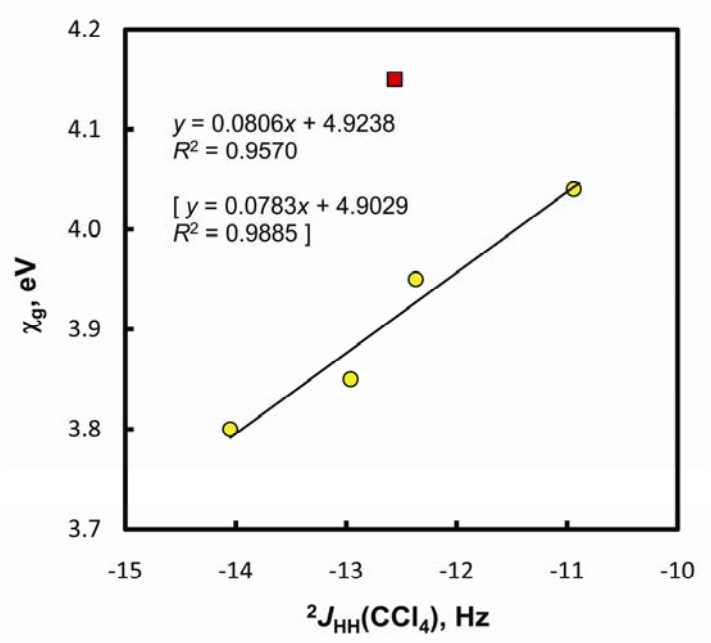

Fig. S8. The group electronegativity χ_g *vs.* experimental $^2J_{HH}(CCl_4)$ couplings; the CMe_4 data point (■) was omitted. Statistics with the χ_g corrected for $-GeMe_3$ (3.88 eV) are in the bracket. The data from Table 3 (main text) were used.

Table S5. Cartesian coordinates for **CMe_4**

[*In vacuo*, the protocol II[‡] used, N_{imag} = 0, E(RB+HF-LYP)= -197.799809 Ha]

Center Number	Atomic Number	Atomic Type	Coordinates (Angstroms) X	Y	Z
1	6	0	0.000000	0.000000	0.000000
2	6	0	0.886699	0.886699	0.886699
3	6	0	-0.886699	-0.886699	0.886699
4	6	0	-0.886699	0.886699	-0.886699
5	6	0	0.886699	-0.886699	-0.886699
6	1	0	1.531597	1.531597	0.279146
7	1	0	0.279146	1.531597	1.531597
8	1	0	1.531597	0.279146	1.531597
9	1	0	-1.531597	-1.531597	0.279146
10	1	0	-1.531597	0.279146	-1.531597
11	1	0	0.279146	-1.531597	-1.531597
12	1	0	-0.279146	-1.531597	1.531597
13	1	0	-1.531597	-0.279146	1.531597
14	1	0	-1.531597	1.531597	-0.279146
15	1	0	-0.279146	1.531597	-1.531597
16	1	0	1.531597	-0.279146	-1.531597
17	1	0	1.531597	-1.531597	-0.279146

[‡] B3LYP/6-31G(*d*,*p*)(C,H)def2-TZVPPD(E)

Table S6. Cartesian coordinates for **$SiMe_4$**

[*In vacuo*, the protocol II used, N_{imag} = 0, E(RB+HF-LYP)= -449.2407721 Ha]

Center Number	Atomic Number	Atomic Type	Coordinates (Angstroms) X	Y	Z
1	14	0	0.000000	0.000000	0.000000
2	6	0	0.000000	0.000000	1.882286
3	6	0	1.774636	0.000000	-0.627429
4	6	0	-0.887318	-1.536880	-0.627429
5	6	0	-0.887318	1.536880	-0.627429
6	1	0	-1.020116	0.000000	2.283291
7	1	0	0.510058	-0.883446	2.283291
8	1	0	0.510058	0.883446	2.283291
9	1	0	1.812669	0.000000	-1.722872
10	1	0	-0.906335	-1.569817	-1.722872
11	1	0	-0.906335	1.569817	-1.722872
12	1	0	2.322727	0.883446	-0.280210
13	1	0	2.322727	-0.883446	-0.280210
14	1	0	-0.396277	-2.453264	-0.280210
15	1	0	-1.926450	-1.569817	-0.280210
16	1	0	-1.926450	1.569817	-0.280210
17	1	0	-0.396277	2.453264	-0.280210

Table S7. Cartesian coordinates for **$GeMe_4$**

[*In vacuo*, the protocol II used, N_{imag} = 0, E(RB+HF-LYP)= -2236.7460606 Ha]

Center Number	Atomic Number	Atomic Type	Coordinates (Angstroms) X	Y	Z
1	32	0	0.000000	0.000000	0.000000
2	6	0	0.000000	0.000000	1.975809
3	6	0	1.862810	0.000000	-0.658603
4	6	0	-0.931405	-1.613241	-0.658603
5	6	0	-0.931405	1.613241	-0.658603
6	1	0	-1.022618	0.000000	2.365508
7	1	0	0.511309	-0.885613	2.365508
8	1	0	0.511309	0.885613	2.365508
9	1	0	1.889349	0.000000	-1.752636
10	1	0	-0.944675	-1.636224	-1.752636
11	1	0	-0.944675	1.636224	-1.752636
12	1	0	2.400658	0.885613	-0.306436
13	1	0	2.400658	-0.885613	-0.306436
14	1	0	-0.433366	-2.521837	-0.306436
15	1	0	-1.967292	-1.636224	-0.306436
16	1	0	-1.967292	1.636224	-0.306436
17	1	0	-0.433366	2.521837	-0.306436

Table S8. Cartesian coordinates for **$SnMe_4$**

[*In vacuo*, the protocol II used, N_{imag} = 0, E(RB+HF-LYP)= -374.045353 Ha]

Center Number	Atomic Number	Atomic Type	Coordinates (Angstroms) X	Y	Z
1	50	0	0.000000	0.000000	0.000000
2	6	0	0.000000	0.000000	2.168123
3	6	0	2.044126	0.000000	-0.722708
4	6	0	-1.022063	-1.770265	-0.722708
5	6	0	-1.022063	1.770265	-0.722708
6	1	0	-1.024413	0.000000	2.551411
7	1	0	0.512207	-0.887168	2.551411
8	1	0	0.512207	0.887168	2.551411
9	1	0	2.064022	0.000000	-1.816296
10	1	0	-1.032011	-1.787495	-1.816296
11	1	0	-1.032011	1.787495	-1.816296
12	1	0	2.576228	0.887168	-0.367557
13	1	0	2.576228	-0.887168	-0.367557
14	1	0	-0.519804	-2.674663	-0.367557
15	1	0	-2.056424	-1.787495	-0.367557
16	1	0	-2.056424	1.787495	-0.367557
17	1	0	-0.519804	2.674663	-0.367557

Table S9. Cartesian coordinates for **$PbMe_4$**

[*In vacuo*, the protocol II used, N_{imag} = 0, E(RB+HF-LYP)= -352.5624235 Ha]

Center Number	Atomic Number	Atomic Type	Coordinates (Angstroms) X	Y	Z
1	82	0	0.000000	0.000000	0.000000
2	6	0	0.000000	0.000000	2.257628
3	6	0	2.128512	0.000000	-0.752543
4	6	0	-1.064256	-1.843346	-0.752543
5	6	0	-1.064256	1.843346	-0.752543
6	1	0	-1.029569	0.000000	2.621891
7	1	0	0.514785	-0.891633	2.621891
8	1	0	0.514785	0.891633	2.621891
9	1	0	2.128753	0.000000	-1.844651
10	1	0	-1.064376	-1.843554	-1.844651
11	1	0	-1.064376	1.843554	-1.844651
12	1	0	2.643538	0.891633	-0.388620
13	1	0	2.643538	-0.891633	-0.388620
14	1	0	-0.549592	-2.735187	-0.388620
15	1	0	-2.093946	-1.843554	-0.388620
16	1	0	-2.093946	1.843554	-0.388620
17	1	0	-0.549592	2.735187	-0.388620

References:

1 L. S. Bartell and W. F. Bradford, *J. Mol. Struct.,* 1977, **37**, 113–126.

2 A. R. Campanelli, F. Ramondo, A. Domenicano and I. Hargittai, *Struct. Chem.,* 2000, **11**, 155–160.

3 E. Csákvári, B. Rozsondai and I. Hargittai, *J. Mol. Struct.,* 1991, **245**, 349–355.

4 M. Nagashima, H. Fuji and M. Kimura, *Bull. Chem. Soc. Jpn.,* 1973, **46**, 3708–3711.

5 T. Oyamada, T. Iijima and M. Kimura, *Bull. Chem. Soc. Jpn.,* 1971, **44**, 2638–2642.

6 W. Lie, D. G. Fedorov and K. Hirao, *J. Phys. Chem. A,* 2002, **106**, 7057–7061.

7 H. Bürger and S. Biedermann, *Spectrochim. Acta A,* 1972, **28**, 2283–2286.

8 C. W. Young, J. S. Koehler and D. S. McKinney, *J. Am. Chem. Soc.,* 1947, **69**, 1410–1415.

9 E. R. Shull, T. S. Oakwood and D. H. Rank, *J. Chem. Phys.,* 1953, **21**, 2024–2029.

10 M. J. Lacey, C. G. Macdonald, A. Pross, J. S. Shannon and S. Sternhell, *Aust. J. Chem.,* 1970, **23**, 1421–1429.

11 F. J. Weigert, M. Winokur and J. D. Roberts, *J. Am. Chem. Soc.,* 1968, **90**, 1566–1569.

12 S. Geer and R. A. Holroyd, *Phys. Rev. B,* 1992, **46**, 5043–5046.